A METHOD OF TUNING ECRIS BEAM TRANSPORT LINES FOR LOW EMITTANCE*

J. W. Stetson#, NSCL/MSU, East Lansing, MI 48824, USA

Abstract

Heavy-ion beams from an ECR-type ion source have been shown to be structurally complex and to have a strong cross-correlation associated with their formation in and extraction from a high magnetic field with a strong sextupole content [1].

The emittances of such beams tend to be unavoidably large (compared to low magnetic field source types) yet because of cross-correlations, resistant to improvement by normal collimation methods [2].

Recent developments with beam from the 14 GHz room temperature ECRIS at the NSCL indicate that careful beam line tuning to pass specific parts of the beam structure can allow greatly reduced 4-dimensional emittances without losing a disproportionate amount of the total intensity.

INTRODUCTION

The National Superconducting Cyclotron Laboratory (NSCL) consists of two cyclotrons in series (the K500 and K1200) [3] which accelerate beams provided by one of two ECR Ion Sources. The primary source is ARTEMIS-A (Advanced Room Temperature Ion Source), which is a modification of the Berkeley AECR source and runs at 14 GHz using permanent sextupole magnets, radial ports and room temperature solenoids. A duplicate source, ARTEMIS-B, has been constructed and is installed on a separate test stand.

The primary operational mode of the accelerators is as a driver for operation of the A1900 particle separator, where stable-nuclei beams of 120-170 MeV/u are impacted on a solid target, with the resulting nuclear fragments collected, purified, and sent as a beam of exotic nuclei to the experimental areas.

MOTIVATION

Generally, from the point of view of the experimental program, the highest possible intensities are desired. The shielding of the production target area would allow for beams of up to 4 kW beam power. Presently, for some beams, final output is limited by the beam intensity from the ion sources. For others, beam powers are limited to about 800 W by losses and resulting heating of extraction elements in the cyclotrons. When the new high intensity ECRIS, SUSI, comes on line in 2009, the loss issue will become more pressing.

An important constraint on any solution to running with higher intensities is that the facility operates by user demand with a run of any particular beam seldom lasting more than a few days. The list of beams available for nuclear science contains 22 different stable isotopes [4]. This great variety of beam types and the short run times requires that tunes also be repeatable, reliable, and quick to optimize.

EXPERIENCE

From nearly the beginning of coupled cyclotron operation in 2001, it was clear that an increase of beam current from the source and subsequent injection did not lead to increased K500 output and overall transmission efficiencies were low. Simple collimation (apertures and a small (8 mm diameter) plasma chamber extraction hole) improved the situation but the resulting beam images seen on phosphor-coated plates inserted into the injection beam line had many undesirable features such as large variations in intensity within the image. Considerable effort on improving injection beam line performance was undertaken, including a major change from magnetic to electrostatic focusing in the initial part of the line and a higher-quality analysis magnet [5, 6]. Better performance through the cyclotrons was achieved as the emittance of the low-energy beam injected into the K500 was reduced.

Artemis-B Beam Tests

In August 2007, the Artemis-B test stand was configured to explore the possibility of making a full 2nd order correction of aberrations in the extracted ECRIS beam due to the sextupole radial confinement field.

The beam line with relevant devices is shown in Figure 1. An electrostatic double-doublet system (DDS) consisting of four quadrupoles and one octupole served as the focusing elements before the 90 degree analysis magnet. Vertical and horizontal steering control is done by offsetting the plate voltages of the first and fourth quadrupoles. A sextupole magnet, rotatable about the beam line axis, was placed between the DDS and the analysis magnet. Calculations had shown that with the DDS set to give a π phase-advance (essentially, a focus) between the source sextupole and the external sextupole, the desired correction could be achieved. An Allison-type scanner was used to measure beam emittances. However, since it is a 2-dimensional device, to achieve some gauge of the higher-order nature of the beam, a pepper-pot-like plate was made to insert into the beam after the analysis magnet, followed by a field-free drift and a viewer plate. (An uncorrelated beam will project an image of the grid hole unchanged except for size, depending on the optical conditions.) The test stand configuration is shown in Figure 1 and the beam used was $^{40}Ar^{7+}$ with an extraction voltage of 20 kV.

*Supported under National Science Foundation Grant PHY-0110253
#stetson@nscl.msu.edu

The correction scheme as tested did not work as anticipated. However, three interesting results were noted that led to a new method of tuning for the beam line injecting into the K500.

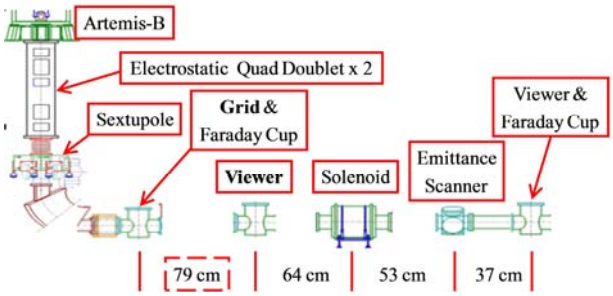

Figure 1: Artemis-B configuration for described tests (not to scale). The grid filters the beam into beamlets that drift 79 cm to a viewer, allowing x-y cross-correlations to be seen easily, as in Fig 2.

First to note is that when tuning the DDS quadrupoles to achieve maximum intensity on the first Faraday cup (without regard for beam quality), the downstream grid projections of the resultant beam were highly structured and contained large correlations. Some of these patterns are shown in Figure 2.

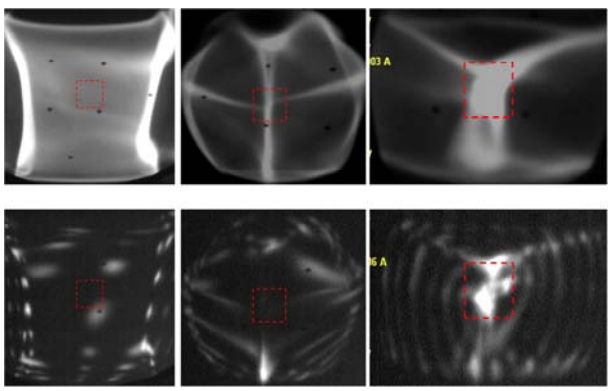

Figure 2: Some $^{40}Ar^{7+}$ beam patterns seen on the first viewer of the Artemis-B test line with various DDS quadrupole settings optimized only for beam intensity (about 120 eμA). The top row is without grid, the bottom row is with the grid inserted. The dashed-line square represents a 1 cm x 1 cm scale in this and subsequent figures.

Figure 3: The Artemis-B grid is placed behind a 25 mm diameter aperture. The grid holes are about 1.5 mm in diameter, and 4 mm between centers.

The grid used for these projections is shown in Figure 3. Hole sizes and spacing are larger than what is used in typical pepper-pot arrangements.

Secondly, it was noted that when the DDS quads were set to values near those calculated to achieve a π phase-advance at the location of the external sextupole, the resulting grid patterns were markedly different. An example is shown in Figure 4. In this case, a major portion of the beam projects the grid pattern 79 cm downstream without major distortion, even with the external sextupole turned off. This indicates that the transmitted portion of beam is without large x-y correlations, i.e. uncorrelated or what is sometimes referred to as laminar [7].

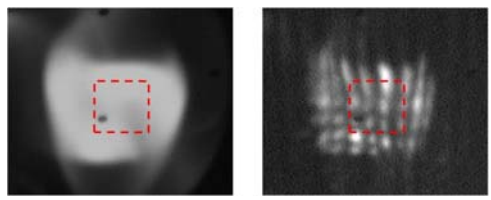

Figure 4: The left-hand image shows the "π phase-advance" tuned $^{40}Ar^{7+}$, 80 eμA beam on the first viewer, without the grid inserted. At right, the grid is inserted, showing a relatively undistorted pattern at the center of a dimmer "cloud".

Lastly, it was also noted that when the beam was tuned in this manner, raising the sextupole captured some of the halo beam, but did not change the "core" in any substantial way, qualitatively hinting that the 2nd order content of this selected part of the beam is low.

Artemis-A Beam Tests

A shutdown of operations in the summer of 2008 allowed an extensive set of tests to be conducted on the K500 injection line. The goal of these tests was to generate the same uncorrelated beam condition seen with Artemis-B, clean up beam tails around the main core of beam, and characterize the results with an Allison-type emittance scanner.

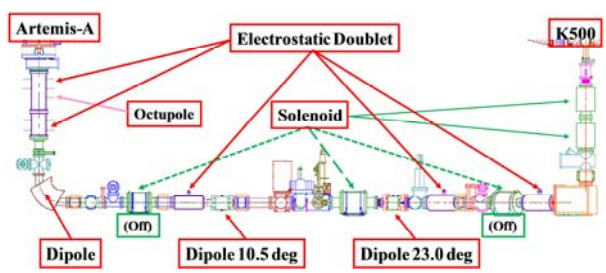

Figure 5: Artemis-A configuration showing the major optical elements.

The major optical elements are shown in Figure 5 and a view with relevant devices is given in Figure 6.

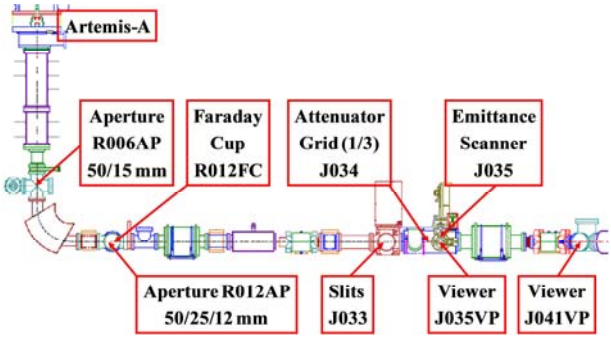

Figure 6: Artemis-A configuration showing the major devices. The 3-digit number within the device name indicates the relative position along the line.

The grid (Fig. 7) is located further downstream than for the Artemis-B line and the drift between the grid and the first viewer (J035VP) is shorter, about 30 cm compared to 79 cm, but still suffices as a qualitative display of beam correlations. In the 2.1 m path between J035VP and the second viewer, J041FP there is a dipole (J039DS) bending 23 degrees and a solenoid (J041SN). With the solenoid set to zero however, this represents an "almost-free" drift since the focusing effects of the dipole are small (negligible in the vertical direction) and the distance from J039DS to J041VP is short.

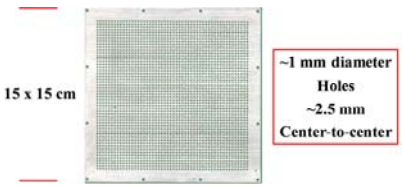

Figure 7: Artemis-A x1/3 attenuator grid, located ~30 cm upstream of the first viewer plate, J035VP.

Using the "π phase-advance" DDS settings from the studies on Artemis-B also gave uncorrelated beam patterns through the J034 grid in the Artemis-A line. Initially, considerable fine-tuning was needed to get both the uncorrelated patterns and low emittance. Accumulated experience with different beams now allows a standard setting for the two quad doublets of the DDS and the beam line quad doublet, J017QA/18QB that gives the desired low-emittance condition and a focus at J035.

The general tuning procedure is as follows:

- With the aperture R006AP in front of the analysis dipole R009DS closed to 15mm, tune the DDS quadrupoles to pass beam through this aperture.
- Use the quadrupole doublet downstream, J017QA/18QB, to focus the beam to a minimum size on viewer J035VP.
- Close R012AP, the aperture after R009DS. Use steering upstream of the aperture to select an intense-looking spot on J035VP.
- Insert the grid at J034 which will cast a pattern on the viewer plate. This pattern should reflect the hole pattern of the grid. If it does not, readjust the DDS quadrupoles and steering to select a different piece of beam that does cast such a pattern.
- With the intermediate solenoid J037SN set to zero, look at the beam on J041VP. Since the beam is a focus/waist at J035VP, the increase in spot size during the drift is directly related to the emittance.
- Opening and closing the apertures at R006 and R012 will show the degree of contamination of the selected beam by other parts following a different path.
- The grid image can be seen on J041VP by raising the J037SN solenoid. Since the grid and the slits at J033 are close together, cutting into the beam with these slits should result in a sharp cut of the grid image seen at J041VP.

Aspects and results of this process are noted below, starting with features in tuning a $^{124}Xe^{20+}$ beam. The first attempt resulted in a distorted grid pattern on J035VP as shown in Figure 8a-Left. (The quad doublet, J017QA/18QB is set to give the minimum spot size on J035VP.) After passing through the drift to J041VP, one sees in Figure 8a-Right a substantial increase in the beam size as well as a highly-structured beam spot.

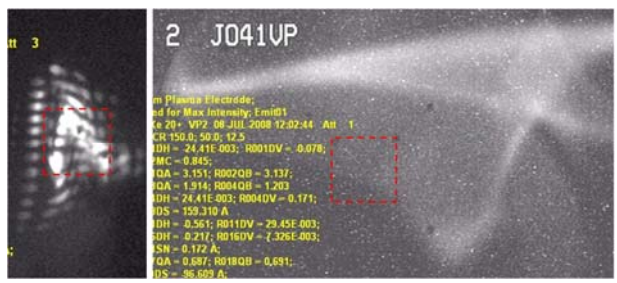

Figure 8a: Images of a $^{124}Xe^{20+}$ beam at J035VP and after the drift to J041VP.

Re-steering and focusing of the DDS quadrupoles, while attempting to keep an organized grid pattern, yet selecting a part of the beam that was small on both viewers, gave the images shown in Figure 8b. The rectilinear grid pattern is visible, the growth of the beam size in the drift is minimal, and the complicated structures seen above, absent.

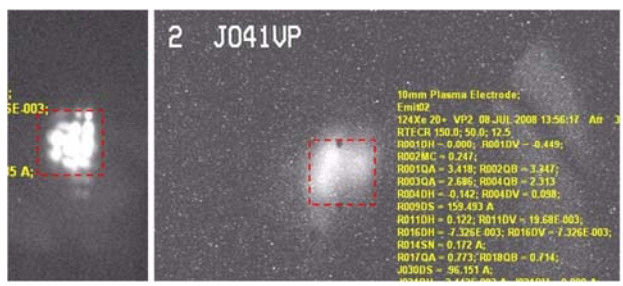

Figure 8b: $^{124}Xe^{20+}$ beam images at J035VP and J041VP as in Figure 8a, but tuned for low emittance.

The implication from the viewer data that the second attempt has reduced emittance in comparison to the first is confirmed by the corresponding emittance scans, given in Figures 9a and 9b.

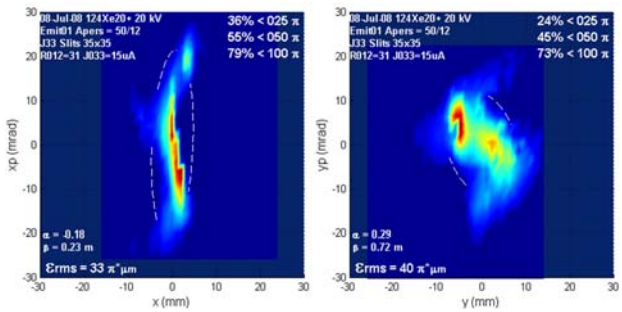

Figure 9a: Horizontal and vertical emittance scans at J035 with a $^{124}Xe^{20+}$ beam tuned as in Fig. 8a. Beam intensity is 31 eμA on the Faraday cup just after the analyzing bend (R012FC) and 15 eμA at the scanner location J033. Resulting emittances are 33 and 40π mm*mrad respectively.

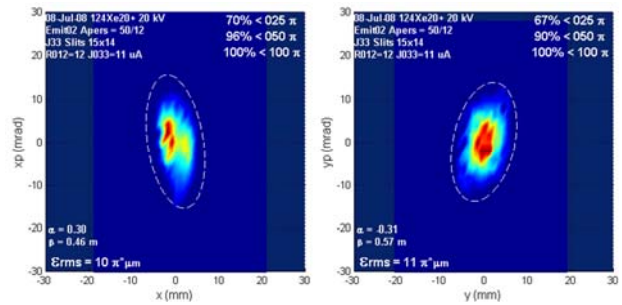

Figure 9b: Horizontal and vertical emittance scans at J035 with a $^{124}Xe^{20+}$ beam tuned as in Fig. 8b. Beam intensity is 12 eμA on R012FC and 11 eμA at J033. Resulting emittances are as calculated are 10 and 11π mm*mrad respectively.

Another test of beam quality is the response of that beam to focusing. In a normal tune transmitting maximum intensity, one manifestation of a cross-dimensional coupling that seems peculiar to ECRIS-produced beam, is that when such a beam is focused to a its smallest size by a solenoid, then over-focused slightly, a star appears [1, 5, 6]. An example of this behavior is shown in Figure 10.

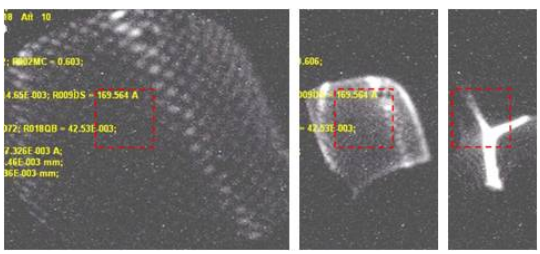

Figure 10: J041VP images. With a $^{40}Ar^{7+}$ beam tuned "normally" through the grid at J034 to a focus/waist at J035VP, the solenoid J037SN between the two viewers is raised from zero to ~110 A.

These low-emittance tunes respond very differently and in a much more desirable way as shown in Figure 11 for a $^{58}Ni^{11+}$ example tuned similarly to the example used for Figures 8b and 9b.

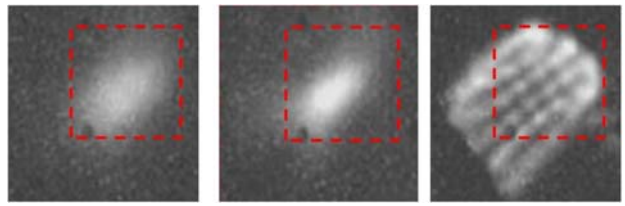

Figure 11a: J041VP images. A low-emittance tuned $^{58}Ni^{11+}$ is passed through the grid at J034 to a focus/waist at J035VP. The solenoid J037SN between the two viewers is raised from 0 to ~100 A. Left is the under-focused condition, center is the minimum spot size, and at right is an over-focused condition.

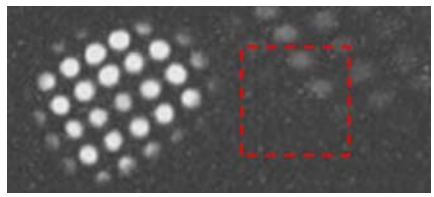

Figure 11b: A J041VP image with the above $^{58}Ni^{11+}$ beam strongly over-focused (J037SN ~ 120A). On the right, a $^{16}O^{3+}$ contaminant is distinctly separated from the main beam.

Because the J033 slits are located close to the grid at J034, a sharp rectilinear grid pattern infers that closing these slits will result in a clean cut. This is shown to be the case in Figure 11c.

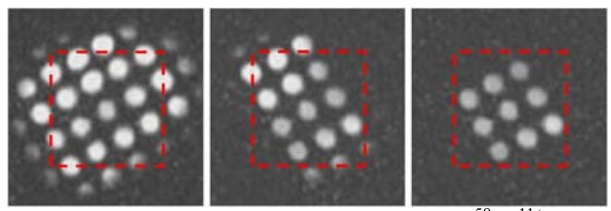

Figure 11c: A J041VP image of the above $^{58}Ni^{11+}$ beam, with the J033 slits open (left), with a vertical gap of 5 mm (middle), and with both the horizontal and vertical gaps set to 5 mm (right).

It is important to remark that if the best piece of the overall beam is selected through focusing and steering upstream of the analysis magnet, that piece is fundamentally uncorrelated and of low emittance. The cuts are not to improve this part of the beam, but serve to cut away other parts of the beam. An example is shown below in Figure 12.

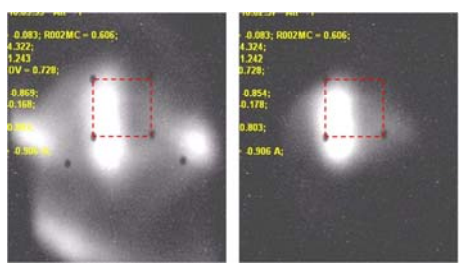

Figure 12: A J041VP image with a $^{40}Ar^{7+}$ beam tuned in the "low emittance" condition. At left, the aperture R012AP = 50 mm diameter, at right, R012AP = 12 mm. The horizontal core of the beam is unaffected; in the vertical direction the cut is a little too severe (which could be eliminated if adjustable slits were used at that location rather than apertures.)

Emittance Scanner Resolution

The resolution of the emittance scanner is given to be 0.5 mm in position and 6.7 mrad in angle [8]. The very low emittances of the beams being produced in these tests often are less than the resolution of this scanner. In particular, positional resolution is adequate given the 5-10 mm spot size typically found at the scanner location. However, when the beam emittances are smaller than about 15π mm*mrad, the measured angle no longer responds to changes in spot size made by focusing only. An example is given in Figure 13.

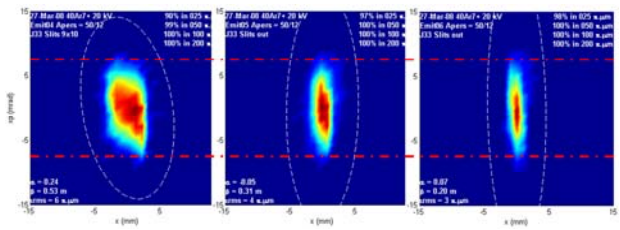

Figure 13: Three emittance scans of the same "low-emittance" tuned $^{40}Ar^{7+}$ beam (selecting about 20% of the maximum available intensity) with the horizontal spot size progressively reduced to a line focus using the quadrupole doublet upstream of the scanner. As the spot size is decreased, the calculated r.m.s. emittance is 8, 6, and 3π mm*mrad respectively. The measured angular divergence is not increasing as it should because it is smaller than what the scanner can presently resolve.

In such cases, common in the "low-emittance" tune mode, the real emittance value is lower than what is calculated from the measurement. Narrower scanner slits will be installed in the future to rectify this issue.

Beam Current

The "low-emittance" tunes result in 70-80% loss in beam intensity measured at the first Faraday cup (R012FC) in comparison to the case where the DDS quadrupole settings and steering are set to give maximum intensity. However, further downstream, this loss is reduced to 25-35% due to the higher losses incurred by the higher-emittance beam. To increase beam intensities, the 8 mm plasma diameter plasma chamber extraction electrode was replaced by one of 10 mm diameter. The beam output went up by about 30-40% and could still be tuned to low-emittance condition very similar to that in the 8 mm case. The net result is that the 10mm/low-emittance tune gives intensities comparable to the 8mm/normal (intensity maximized) tune at the last injection line faraday cup before the K500, but with much higher 2-d brightness. The improvement would be even greater if comparing 4-d volumes, since, as shown above, the normal beams exhibit complicated x-y coupling that are essentially absent in these low-emittance tunes.

CONCLUSIONS

Results of these tests can be summarized as follows:

- Beams of $^{40}Ar^{7+}$, $^{58}Ni^{11+}$, $^{78}Kr^{11+}$, and $^{124}Xe^{20+}$ were extensively tested and showed very similar optical properties.
- A bright beam core exists that has minimal, if any, cross-correlations.
- This core has about 20-30% of the intensity of a beam tuned for maximum current.
- Measured 2-d emittances are reduced by at least a factor of 3-5 over that of the full beam. Higher-resolution scans will be needed to fully quantify the improvements.
- Settings of the first quadrupole focusing elements scale by extraction voltage very precisely between the different ion beams.
- The minimal x,y beam correlations that result from this technique allow clean slit cuts.
- Changing the plasma chamber electrode diameter from 8mm to 10mm increased both overall and "low emittance" output by 30-40%, without significantly degrading the quality of the "low-emittance" tuned beam.

ACKNOWLEDGEMENTS

The author wishes to thank D. Cole, M. Doleans, G. Machicoane, L. Tobos, P. Zavodszky at NSCL and P. Spädtke at GSI for their contributions.

REFERENCES

[1] P. Spädtke, R. Lang, J. Mäder, J. Rossbach, K. Tinschert, J. Stetson, 17th Int. Workshop on ECR Ion Sources, Lanzhou, China (2007), p. 192.
[2] J. Stetson, P. Spädtke, IEEE Proc. of PAC07, Albuquerque, N.M., USA (2008).
[3] F. Marti, P. Miller, D. Poe, M. Steiner, J. Stetson, and X.Y. Wu, in Cyclotrons and their Applications 2001, AIP Conf. Proc. 600 (2001) p. 64.
[4] www.nscl.msu.edu/exp/propexp/beamlist .
[5] J. Stetson, G. Machicoane, P. Miller, M. Steiner, P. Zavodszky, in Proc. of LINAC06, 2007, p. 352.
[6] J. Stetson, G. Machicoane, P. Miller, M. Steiner, X. Wu at the 18th Intl. Conf. on Cyclotrons and their Applications, Catania, Italy, 2007, p. 340.
[7] S. Humphries, *Charged Particle Beams*, 1990, p. 80.
[8] G. Machicoane, M. Doleans, G. Humenik, P. Miller, M. Steiner, J. Stetson, X. Wu, P. Zavodszky, Q. Zhao, 17th Int. Workshop on ECR Ion Sources, Lanzhou, China (2007), p. 187.